Perfectly matched multiscale simulations

Albert C. To and Shaofan Li*
Department of Civil and Environmental Engineering, University of California, Berkeley, California, 94720 USA
(Received 10 November 2004; revised manuscript received 2 May 2005; published 6 July 2005)

A multiscale method is proposed. It combines the so-called bridging scale method and the perfectly matched layer method to form a robust and versatile multiscale algorithm. The method can efficiently eliminate the spurious reflections/diffractions from the artificial atomistic/continuum interface by matching the impedance at the interface of the molecular dynamic region and the perfectly matched layer. Moreover, it is shown in this paper that the method can capture anharmonic interaction among nonuniformly distributed atoms in a local region.

DOI: 10.1103/PhysRevB.72.035414 PACS number(s): 46.15.−x, 02.70.Ns, 05.10.−a, 45.10.−b

I. INTRODUCTION

It has become a general consensus now that within the near future first-principle-based simulations will still have insurmountable difficulties to simulate a nanoscale thermal mechanical system because even a small nanoscale thermal mechanical system may consist of more than billions of degrees of freedom (10^9–10^{12}) and have a typical time scale at femtoseconds (10^{-15} s).

An attractive approach is the so-called multiscale simulation, which uses first-principle-based methods, such as molecular dynamics (MD) simulations or even quantum mechanics (QM) based simulations, in a small local area that contains localized inhomogeneities (defects), while it uses continuum approach to model the rest of the remaining (but vast) area. During the simulation, mechanical and thermodynamic information such as energy, heat, and configuration force (energy momentum flux) interchange between atomistic scale and continuum scale. Coupling these complicated processes in a concurrent multiscale simulation is the challenge of the emerging nanoscale computational mechanics. If the challenge is successfully met, the method can be used to simulate, for example, DNA supercoiling, crack initiation, and dislocation motion.

The main difficulty in a concurrent multiscale simulation is the spurious reflection of phonons due to the change of physical modeling as well as spatial resolution. The spurious reflection prevents any meaningful evaluation of temperature fluctuation in the local region, and hence any meaningful multiscale simulation. A few techniques have been proposed to solve this problem. We would like to mention the several front runners of the current multiscale simulation research: (1) Cai *et al.*s generalized Langevin approach,[1] (2) E's optimal local matching procedure,[2–4] and (3) Liu and his coworkers' bridging scale method.[5–8]

In this paper, we propose an alternative multiscale approach called the perfectly matched multiscale simulation (PMMS). The new approach incorporates Berenger's perfectly matched layer (PML) into a local MD simulation[9] to eliminate the spurious reflections at the atomistic-continuum boundary during the fine scale part of the multiscale simulation.

The rest of the paper is arranged as follows: The general ideas and procedures of PMMS are presented in Sec. II. The multiscale decomposition of displacement fields is discussed in Sec. III. In Sec. IV, a PML is formulated for an MD simulation, and, in Sec. V, implementation of the PMMS algorithm is given and several examples of nonlinear wave propagation are presented. A few concluding remarks are made in Sec. VI.

II. THE BASIC IDEAS OF PMMS

A one-dimensional schematic illustration of the PMMS is shown in Fig. 1. A continuum simulation is performed for the whole domain of interest, while an MD simulation is only limited to the pure MD region and the MD-PML region. The MD simulation is performed to provide information from atomistic scale to the continuum level, whereas the continuum simulation provides coarse scale information for the MD-PML region. Typically, the continuum simulation is performed by using the finite element method (FEM or FE) based on the quasi-continuum modeling.[10] The purpose of the MD-PML region is to absorb any waves leaving the pure MD region so they will not introduce any artificial reflections.

Since the temporal resolution in the MD simulation is much smaller than that in the FE, the MD simulation runs independently at each fine time step except when the coarse time step of the FE coincides with the fine step of the MD simulation. At this coincidence, the fine scale part of the MD displacement is added to the FE nodal displacement for each node in the MD region for the computation of internal force in the FE region. At the same time step, the coarse scale part of the displacement and velocity of each atom in the MD-PML region is approximated by the interpolated FE displacement and velocity for the corresponding boundary atom. This

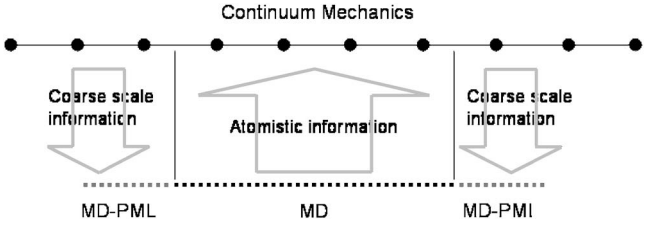

FIG. 1. The schematic illustration of PMMS in 1D.

completes the information exchange between the MD and the continuum regions. The formulation of the fine-coarse scale decomposition and the PML will be presented in the following two sections, respectively.

The following summarizes the procedure of PMMS:

MD (pure MD+MD-PML) region update:

1. At each fine step, update displacement, velocity, and acceleration in the MD region.

2. When the coarse step coincides the fine step, the coarse scale part of the MD displacement and velocity of each atom in the MD-PML region is approximated by the interpolated FE displacement for the corresponding atom.

FE region update:

1. At each coarse step, update displacement and velocity.

2. Add the fine scale part of the MD displacement to the displacement for each FE node in the pure MD region.

3. Update internal force and acceleration.

The numerical implementation of these steps will be given in Sec. V.

III. FINE-COARSE SCALE DECOMPOSITION

The key issue in multiscale simulations is how to couple the same physical quantity (i.e., displacement) from the computations of different scales by using different modeling schemes. In this paper, we treat the molecular dynamics (MD) simulation as the first principle-based method and seek to replace the MD computation by coarse scale finite element computation in a less crucial region in order to improve computational efficiency while maintaining sufficient accuracy compared to an MD only calculation. In the local MD region, information will need to be exchanged between the MD and FE calculations. In the following, a linear relation is derived between the MD displacement and the FE displacement to allow exchange between the two regions during a PMMS simulation.

We adopt the Lagrangian mechanics description of molecular dynamics (MD):

$$L(\mathbf{q},\dot{\mathbf{q}}) = \tfrac{1}{2}\dot{\mathbf{q}}^T\mathbf{M}_A\dot{\mathbf{q}} - U(\mathbf{q}) + \mathbf{f}_{ext}^T\mathbf{q}, \tag{1}$$

where $\mathbf{q}$ is the MD displacement of the discrete atoms, $\mathbf{M}_A$ is the mass matrix, U is the potential energy function, and $\mathbf{f}_{ext}$ is the external force.

In principle, the total displacement field of the exact solution can be written as the sum of fine scale and coarse scale displacements:

$$\mathbf{u} = \mathbf{u}' + \bar{\mathbf{u}}, \tag{2}$$

where $\mathbf{u}$ equals $\mathbf{q}$ at the atomic positions.

The above decomposition is not unique. Assume that the exact solution of an MD simulation exists. A fine scale solution can be determined if a coarse scale solution has been assigned.

In this work, the coarse scale solution is taken as an FEM solution based on the quasi-continuum modeling. Therefore, the coarse scale displacement obtained by the FE at the initial positions of the atoms can be written as

$$\bar{\mathbf{u}} = \mathbf{N}\mathbf{d}, \tag{3}$$

where $\mathbf{d}$ is the nodal displacement and $\mathbf{N}$ is a matrix that consists of shape functions that interpolate the nodal displacement at each initial atomic position. The Lagrangian of the FE can then be defined as

$$\bar{L}(\mathbf{d},\dot{\mathbf{d}}) = \tfrac{1}{2}\dot{\mathbf{d}}^T\mathbf{M}\dot{\mathbf{d}} - \bar{U}(\mathbf{N}\mathbf{d}) + \mathbf{f}_{ext}^T(\mathbf{N}\mathbf{d}), \tag{4}$$

where $\mathbf{M}=\mathbf{N}^T\mathbf{M}_A\mathbf{N}$ is the mass matrix.

To obtain a relationship between the MD displacement $\mathbf{q}$ and the nodal displacement $\mathbf{d}$ in FE in the pure MD region, we assume that a linear mapping $\mathbf{P}$ maps the MD displacement $\mathbf{q}$ to the coarse scale displacement $\bar{\mathbf{u}}$:

$$\bar{\mathbf{u}} \approx \mathbf{P}\mathbf{q}, \tag{5}$$

where the approximation symbol indicates that such projection may not be exact, because first the linear projection operator may not be accurate, and second it is possible that the FEM solution may not be completely contained in the solution space of $\mathbf{q}$.

We can then write the MD displacement as

$$\mathbf{q} = \mathbf{P}\mathbf{q} + (\mathbf{I}-\mathbf{P})\mathbf{q}. \tag{6}$$

Define $\mathbf{Q} := \mathbf{I}-\mathbf{P}$. This suggests that inside the MD zone, the exact displacement field may be approximated as

$$\mathbf{u} \approx \mathbf{N}\mathbf{d} + \mathbf{Q}\mathbf{q}, \tag{7}$$

where $\mathbf{Q}\mathbf{q}$ is used to approximate the fine scale solution of a FEM node inside the MD zone, i.e., $\mathbf{u}' \approx \mathbf{Q}\mathbf{q}$, and hence total solution for a FEM node inside the MD zone. This cannot be achieved without the coarse scale FE calculation inside the MD zone. Note that inside the MD zone, a FEM node does not necessarily coincide with an atom's position, thereby one cannot directly use the MD solution $\mathbf{q}$ to find $\mathbf{u}$ without interpolation.

The coarse scale calculation based on the FE is an approximation to the MD calculation, but it should be close to it. Thus we find the projection map $\mathbf{Q}$ by minimizing the difference of the MD and the FE Lagrangians,

$$C(\mathbf{d},\dot{\mathbf{d}}) = \min_{\mathbf{d},\dot{\mathbf{d}}}[L(\mathbf{q}(\mathbf{d}),\dot{\mathbf{q}}(\dot{\mathbf{d}})) - \bar{L}(\mathbf{d},\dot{\mathbf{d}})]. \tag{8}$$

Substituting in the respective Lagrangians, we obtain

$$C(\mathbf{d},\dot{\mathbf{d}}) = \min_{\mathbf{d},\dot{\mathbf{d}}}\Bigg[\tfrac{1}{2}(\mathbf{N}\dot{\mathbf{d}}+\mathbf{Q}\dot{\mathbf{q}})^T\mathbf{M}_A(\mathbf{N}\dot{\mathbf{d}}+\mathbf{Q}\dot{\mathbf{q}}) - U(\mathbf{N}\mathbf{d}+\mathbf{Q}\mathbf{q}) + \mathbf{f}_{ext}^T(\mathbf{N}\mathbf{d}+\mathbf{Q}\dot{\mathbf{q}}) - \frac{1}{2}\dot{\mathbf{d}}^T\mathbf{M}\dot{\mathbf{d}} + \bar{U}(\mathbf{N}\mathbf{d}) - \mathbf{f}_{ext}^T(\mathbf{N}\mathbf{d})\Bigg]. \tag{9}$$

Let partial derivatives of the objective function $C(\mathbf{d},\dot{\mathbf{d}})$ to zero,

$$\frac{\partial C}{\partial \mathbf{d}} = -\mathbf{N}^T\frac{\partial U(\mathbf{q})}{\partial \mathbf{q}} + \mathbf{f}_{ext} + \mathbf{N}^T\frac{\partial \bar{U}(\bar{\mathbf{u}})}{\partial \bar{\mathbf{u}}} - \mathbf{f}_{ext} = 0, \tag{10}$$

which implies that we shall choose $U(\mathbf{q})=\bar{U}(\bar{\mathbf{u}})$. In addition, we also have

$$\frac{\partial C}{\partial \dot{\mathbf{d}}} = \mathbf{N}^T\mathbf{M}_A\mathbf{N}\dot{\mathbf{d}} + \mathbf{N}^T\mathbf{M}_A\mathbf{Q}\dot{\mathbf{q}} - \mathbf{N}^T\mathbf{M}_A\mathbf{N}\dot{\mathbf{d}} = 0, \tag{11}$$

which yields

$$\dot{\mathbf{d}} = \mathbf{M}^{-1}\mathbf{N}^T\mathbf{M}_A\dot{\mathbf{q}} \tag{12}$$

where we have made use of Eq. (7):

$$\mathbf{N}\dot{\mathbf{d}} = (\mathbf{I} - \mathbf{Q})\dot{\mathbf{q}}. \tag{13}$$

Comparing (13) with (12), one sees that

$$\mathbf{Q} = \mathbf{I} - \mathbf{N}\mathbf{M}^{-1}\mathbf{N}^T\mathbf{M}_A. \tag{14}$$

It is simple to check that $\mathbf{QQ}=\mathbf{Q}$, which means that $\mathbf{Q}$ is a projector. Also, the projector $\mathbf{P}$ is

$$\mathbf{P} = \mathbf{N}\mathbf{M}^{-1}\mathbf{N}^T\mathbf{M}_A. \tag{15}$$

Although the linear projectors $\mathbf{Q}$ and $\mathbf{P}$ obtained here are identical to those obtained for the bridging scale method,[6] the derivation here is physically better justified by minimizing the difference between the Lagrangian of the MD and the FE. Also, a linear mapping is assumed in this work; however, a nonlinear operator can also be assumed, but analytical results will be difficult to obtain, and the resulting operator may only be obtained numerically.

More precise physical meaning can be attached to the terms "fine scale displacement" and "coarse scale displacement." Say, the nodal spacing in the FE simulation is h and the atomic spacing is h_a, and $h > h_a$ is assumed as usual. The minimum wavelength that the FE can support is $\lambda_{min} \approx 4h$ while the MD simulation can support down to a wavelength of $\lambda^a_{min} \approx 4h_a$. According to the decomposition in Eq. (2), the coarse scale displacement $\bar{\mathbf{u}}$ calculated by the FE includes all wavelengths that are greater than λ_{min} while the fine scale displacement $\mathbf{u}'$ calculated by the MD simulation represents wavelengths between λ^a_{min} and λ_{min}. These more precise definitions will help to explain the ideas of PMMS.

IV. PERFECTLY MATCHED LAYER

The perfectly matched layer (PML) was developed by Berenger[9] to damp electromagnetic waves without introducing artificial reflections at the boundary of the model domain. The technique has since been applied to many different transient problems and is highly successful since it damps body waves and evanescent waves at all frequencies except at zero frequency with minimal reflections.[11–14] It can also be applied to anisotropic and inhomogeneous media, and its implementation is quite simple. The PML equation for the molecular dynamics (MD) simulation is derived below and it shows that anharmonic waves in MD can also be treated.

We begin the derivation with the classical Newton's second law:

$$\mathbf{F}_\alpha = m\ddot{\mathbf{q}}_\alpha = -\frac{\partial U(\mathbf{r}^N)}{\partial \mathbf{r}_\alpha}, \tag{16}$$

where the subscript α denotes the αth atom, and U is the potential function that depends on the positions $\mathbf{r}^N$ of the Nth atom that interact with the αth atom. In Cartesian coordinates, the forces in each coordinate are independent of those in another coordinate; it is sufficient to look at, say, the x coordinate, and Newton's law becomes

$$m_\alpha\ddot{q}_\alpha = -\frac{\partial U(\mathbf{r}^N)}{\partial x_\alpha}. \tag{17}$$

Denote

$$\mathcal{S} := -\int U\, dx_\alpha. \tag{18}$$

Equation (17) can be rewritten as

$$m_\alpha\ddot{q}_\alpha = \frac{\partial^2\mathcal{S}}{\partial x_\alpha^2}. \tag{19}$$

This equation can be split into two first-order equations by defining an auxiliary variable:

$$\frac{\partial p_\alpha}{\partial x_\alpha} := \dot{q}_\alpha. \tag{20}$$

Its dual equation is

$$\dot{p}_\alpha = \frac{1}{m_\alpha}\frac{\partial \mathcal{S}}{\partial x_\alpha}. \tag{21}$$

One constructs a perfectly matched layer by converting the real coordinates into complex coordinates as a function of frequency ω. In other words, the following operation is performed to the dual equations (20) and (21) to convert the equations

$$\partial x_\alpha \rightarrow \left(1 + \frac{d(x_p)}{-i\omega}\right)\partial x_\alpha, \tag{22}$$

where $d(x_p)$ is the damping function that controls the damping with propagating distance and x_p is the distance away from the MD and PML boundary. Applying the coordinate stretching to the Fourier transformed dual equations, one can obtain

$$-i\omega\left(1 + \frac{d(x_p)}{-i\omega}\right)\hat{q}_\alpha = \frac{\partial \hat{p}_\alpha}{\partial x_\alpha}, \tag{23}$$

$$-i\omega\left(1 + \frac{d(x_p)}{-i\omega}\right)\hat{p}_\alpha = \frac{1}{m_\alpha}\frac{\partial \hat{\mathcal{S}}}{\partial x_\alpha}, \tag{24}$$

where $\hat{f}$ denotes the Fourier transform of f. Performing inverse transform, the perfectly matched layer equations are obtained:

$$\dot{q}_\alpha = \frac{\partial p_\alpha}{\partial x_\alpha} - d(x_p)q_\alpha, \tag{25}$$

$$\dot{p}_\alpha = -\frac{U}{m_\alpha} - d(x_p)p_\alpha. \tag{26}$$

Combining (25) and (26) yields the modified equation of motion for PML:

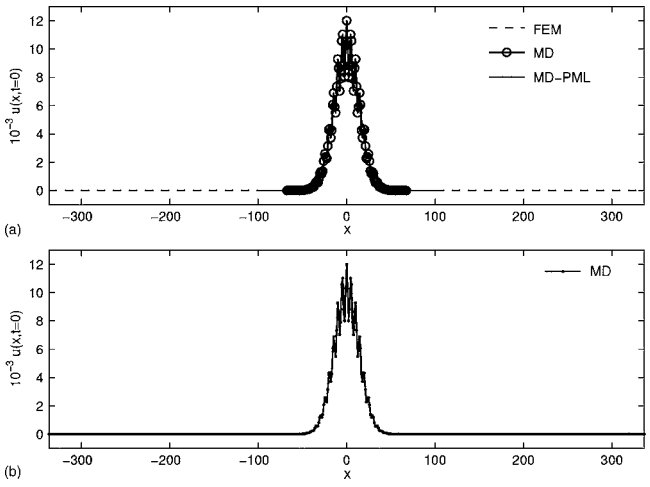

FIG. 2. Initial displacement for the 1D lattice problem with Lennard-Jones potential function obtained by (a) PMMS and (b) full MD simulation.

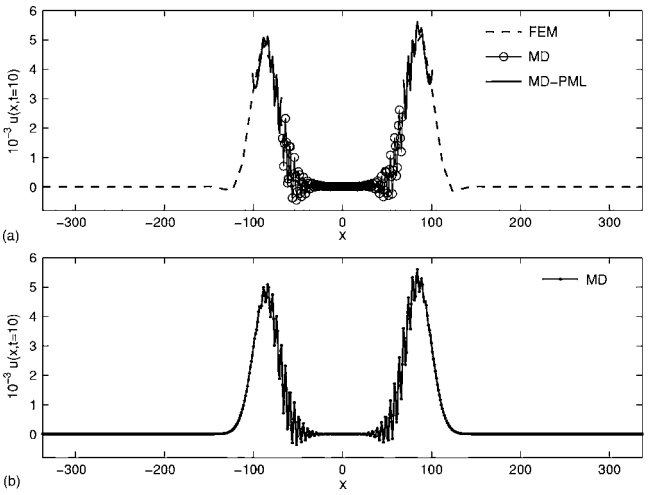

FIG. 3. Displacement at $t=10$ for the 1D lattice problem with the Lennard-Jones potential function obtained by (a) PMMS and (b) full MD simulation.

$$m_\alpha \ddot{q}_\alpha = -\frac{\partial U(\mathbf{r}^N)}{\partial x_\alpha} - m_\alpha d(x_p)^2 q_\alpha - 2m_\alpha d(x_p)\dot{q}_\alpha. \quad (27)$$

Note that the effect of coordinate stretch is not equivalent to simply adding a damping term; it also changes the stiffness of the discrete system in the PML zone in order to create an optimal match for impedance forces.

Since the derivation of the MD-PML equation does not involve or require any linearization of the atomistic potential, the PML technique can handle spurious reflections of both harmonic waves and anharmonic waves. Note that when the damping function $d(x_p)=0$, the MD-PML equation (27) recovers the original Newton's equation.

In this paper, we adopt the semi-empirical damping function proposed by Collino and Tsogka[15] :

$$d(x_p) = d_0 \frac{x_p^2}{\delta}, \quad (28)$$

$$d_0 = \log\left(\frac{1}{R}\right)\frac{3V}{2\delta}, \quad (29)$$

where δ is the PML thickness, R is a free parameter less than unity, and V is the wave velocity.

The success of the absorbing boundary conditions has very important implications in PMMS since artificial reflections are of primary concern. PML formulation for other partial differential equations can be shown to be nonreflecting at the boundary in its continuum form, but once the equations are discretized as in finite difference or finite element methods, artificial reflected waves may exist due to discretization. Nevertheless, the PML is still much better than absorbing boundary conditions that use linear damping mechanisms that is only effective in a certain range of frequencies while the PML formulation damps waves of all frequencies except zero frequency (static). For elastodynamic problems that use the PML in finite difference, the PML only requires five to ten layers of nodes for 2D and 3D problems to prevent any artificial reflections. The current PML formulation for molecular dynamics is inherently discretized since the potential function U depends on the neighboring atoms, but from the discussion above, the PML for molecular dynamics should also perform well as will be seen.

V. IMPLEMENTATION

The implementation of the PMMS is much simpler than other existing multiscale methods. As stated in Sec. II, the whole simulation consists of running the FE at coarse time steps Δt and running the MD simulation at fine time steps $\Delta t_m = \Delta t/m$, where m is an integer. Therefore, at the nth step of the FE, information from the $j=(n\times m)$th step of the MD calculation is projected onto the FE nodes for FE update. Immediately after the FE update, information is interpolated at the MD boundary atoms. We use the mixed time integration scheme pioneered by Liu and Belytschko for solving dynamic fluid-structure problems.[16]

The Verlet algorithm is chosen for the MD (including the PML) simulation update at the jth step:

$$\mathbf{q}^{j+1} = \mathbf{q}^j + \Delta t_m \dot{\mathbf{q}}^j + \tfrac{1}{2}\Delta t_m^2 \ddot{\mathbf{q}}^j, \quad (30)$$

$$\dot{\mathbf{q}}^{j+1/2} = \dot{\mathbf{q}}^j + \tfrac{1}{2}\Delta t_m \ddot{\mathbf{q}}^j, \quad (31)$$

$$\ddot{\mathbf{q}}^{j+1} = \mathbf{M}_A^{-1}\left(-\frac{\partial U}{\partial \mathbf{q}} - \mathbf{M}_A\mathbf{D}^2\mathbf{q}^{j+1} - 2\mathbf{M}_A\mathbf{D}\dot{\mathbf{q}}^{j+1/2} + \mathbf{f}_{ext}^j\right), \quad (32)$$

$$\dot{\mathbf{q}}^{j+1} = \dot{\mathbf{q}}^{j+1/2} + \tfrac{1}{2}\Delta t_m \ddot{\mathbf{q}}^{j+1}, \quad (33)$$

where the matrix $\mathbf{D}$ is a diagonal matrix consisting of the damping function d as defined in (28), which is set to zero in the pure MD region. Note that Eq. (32) is the discretized version of (27) for all the atoms. At the nth step of the FE update, we have

$$\mathbf{d}^{n+1} = \mathbf{d}^n + \Delta t \mathbf{v}^n + \tfrac{1}{2}\Delta t^2 \mathbf{a}^n, \quad (34)$$

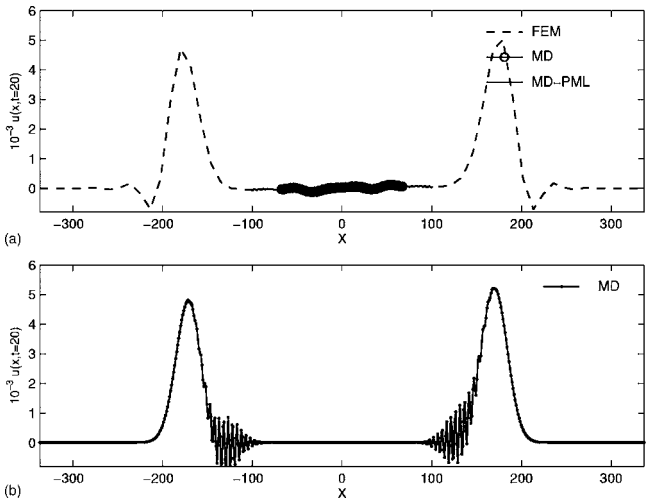

FIG. 4. Displacement at $t=20$ for the 1D lattice problem with Lennard-Jones potential function obtained by (a) PMMS and (b) full MD simulation.

$$\mathbf{a}^{n+1} = \mathbf{M}^{-1}\mathbf{N}^T\mathbf{f}(\mathbf{N}\mathbf{d}^{n+1} + \mathbf{Q}\mathbf{q}^{j+1}), \tag{35}$$

$$\mathbf{v}^{n+1} = \mathbf{v}^n + \tfrac{1}{2}\Delta t(\mathbf{a}^n + \mathbf{a}^{n+1}). \tag{36}$$

At the same $j=(m\times n)$th fine step, the coarse scale part of the MD displacements and velocities are approximated by the FE displacements and velocities through interpolation for only the atoms in the PML region:

$$\mathbf{q}^{j+1} = \mathbf{N}\mathbf{d}^{n+1} + \mathbf{Q}\mathbf{q}^{j+1}, \tag{37}$$

$$\dot{\mathbf{q}}^{j+1} = \mathbf{N}\mathbf{v}^{n+1} + \mathbf{Q}\dot{\mathbf{q}}^{j+1}, \tag{38}$$

where $\mathbf{Q}\mathbf{q}^{j+1}$ and $\mathbf{Q}\dot{\mathbf{q}}^{j+1}$ are the fine scale part of the displacements and velocities in the PML region having been calculated in Eqs. (30) and (33). Equations (37) and (38), in effect, allow the damping of all the fine scale waves in the PML region while maintaining sufficient accuracy at the boundary of the pure MD region.

To demonstrate the proposed perfectly matched multiscale method, numerical simulations are carried out for the following one-dimensional problem. Consider a one-dimensional lattice. The Lennard-Jones (LJ) potential function is used for the nearest neighboring atom interaction:

$$U(r_{ij}) = 4\left[\left(\frac{1}{r_{ij}}\right)^{12} - \left(\frac{1}{r_{ij}}\right)^{6}\right], \tag{39}$$

where r_{ij} the position difference between atom i and j. An initial displacement is given,

$$u(x,t=0) = \begin{cases} A\frac{e^{-(x/\sigma)^2}-u_c}{1-u_c}\left[1+b\cos\left(\frac{2\pi x}{H}\right)\right], & |x| \leqslant L_c, \\ 0, & |x| > L_c, \end{cases} \tag{40}$$

which is a Gaussian pulse of amplitude A and width σ. The pulse is truncated at $x=\pm L_c$. The initial displacement is plotted in Fig. 2 in the 1D lattice. The lattice is modeled by 60 elements in the FE simulation, 181 atoms spaced at $2^{1/6}$ in the full MD simulation, of which 60 atoms are in the MD-PML region. In addition, the fine and coarse time steps are $\Delta t_m=0.002$ and $\Delta t=0.1$, respectively. The values used for the parameters in Eq. (40) are $\sigma=20.0$, $H=\sigma/4$, $A=0.01$, $b=0.2$, and $L_c=4\sigma$.

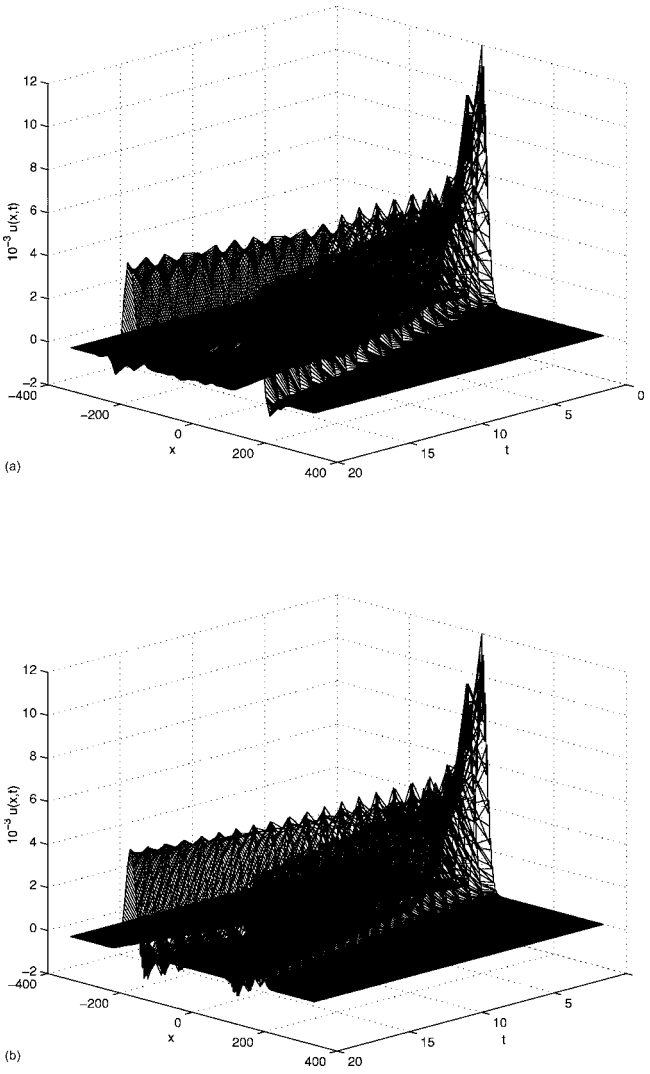

FIG. 5. Time-displacement history for the 1D lattice problem with Lennard-Jones potential function obtained by (a) PMMS and (b) MD.

Figures 3 and 4 show the displacement at $t=10$ and $t=20$ coarse time steps, respectively. There are very few waves reflected back into the pure MD region when the waves propagate into the uncoupled FE region. The waves that pass into the MD-PML region from the pure MD region are being damped quickly with very few reflections. The time-displacement histories for PMMS and full MD simulation are plotted in Fig. 5, and their general shapes agree well. A quantitative analysis of the current method is performed by plotting the Fourier spectrum of the displacement-time history of the incident wave and reflected wave measured in the MD region at $x=56.12$ and that of the transmitted wave measured in the FE region at $x=101.02$, as shown in Fig. 6. The energy of the incident wave is concentrated at three peaks in the figure, and the transmitted wave spectrum captures the

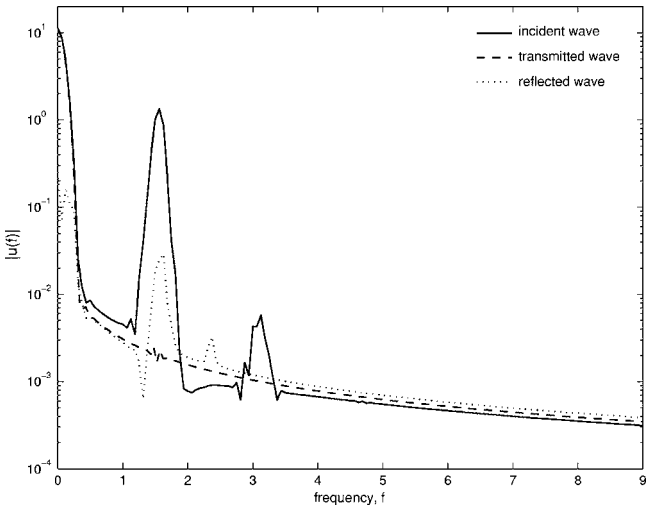

FIG. 6. Fourier spectrum of the incident wave in the pure MD region, the reflected wave in the pure MD region after reaching the handshake region, and the transmitted wave in the FE region corresponding to the Lennard-Jones example.

lowest frequency peak almost exactly, but completely misses the second and third peaks, which represent the higher frequency waves at the back end of the main wave front seen clearly in Fig. 4 at around $x=\pm 120$. The minimum wavelength that the FE region can support is $\lambda_{min}=40$ and the wave travels at velocity $v=9$, and thus the highest frequency that the FE region can support is approximately $f_{max}=v/\lambda_{min}=0.23$, which is right after the first peak. In the full MD simulation, there is no reflected wave, however, in PMMS the reflected wave is approximately two orders of magnitude less than the incident wave in amplitude, but resembles the incident wave in frequency content for the first two peaks.

In the second example, the collision of a pair of sine-Gordon solitons is considered. The potential function used in this case is

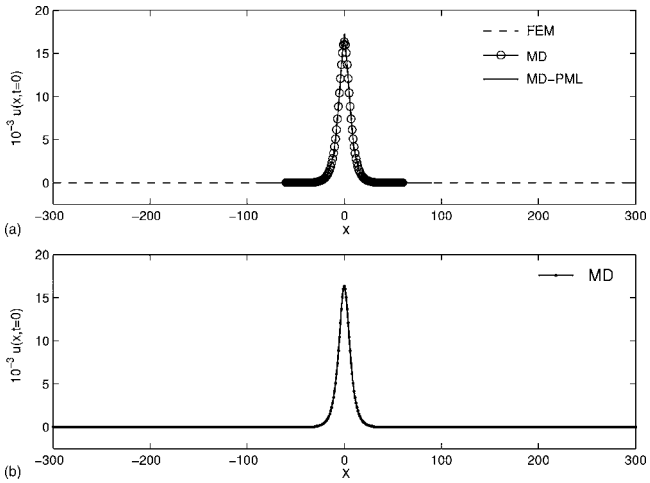

FIG. 7. Initial displacement for the 1D lattice problem with sine-Gordon potential function obtained by (a) PMMS and (b) full MD simulation.

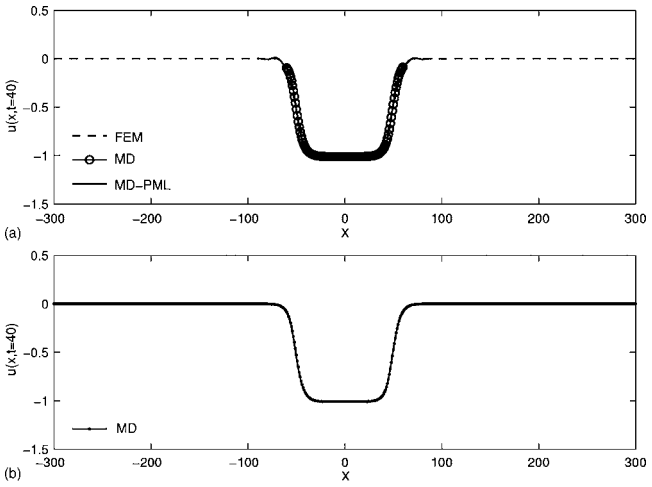

FIG. 8. Displacement at $t=40$ for the 1D lattice problem with sine-Gordon potential function obtained by (a) PMMS and (b) full MD simulation.

$$U(r_{ij}) = \tfrac{1}{2}r_{ij}^2 + 1 - \cos(r_{ij} - r_0), \tag{41}$$

where r_0 is the equilibrium atomic spacing. We only consider the nearest neighboring interaction among atoms.

The initial displacement and velocity used for the collision of two solitons are

$$u(x,0) = 4\tan^{-1}\left[\exp\left(\frac{b(x+x_0)}{\sqrt{1-\beta^2}}\right)\right] + 4\tan^{-1}\left[\exp\left(\frac{b(-x+x_0)}{\sqrt{1-\beta^2}}\right)\right], \tag{42}$$

$$v(x,0) = -4\left(\frac{\frac{b\beta}{\sqrt{1-\beta^2}}\exp\left(\frac{b(x+x_0)}{\sqrt{1-\beta^2}}\right)}{1+\exp\left(\frac{b(x+x_0)}{\sqrt{1-\beta^2}}\right)^2}\right) - 4\left(\frac{\frac{b\beta}{\sqrt{1-\beta^2}}\exp\left(\frac{b(-x+x_0)}{\sqrt{1-\beta^2}}\right)}{1+\exp\left(\frac{b(-x+x_0)}{\sqrt{1-\beta^2}}\right)^2}\right). \tag{43}$$

where the initial displacement field in a 1D lattice is plotted in Fig. 7. The configuration of the 1D lattice is identical to

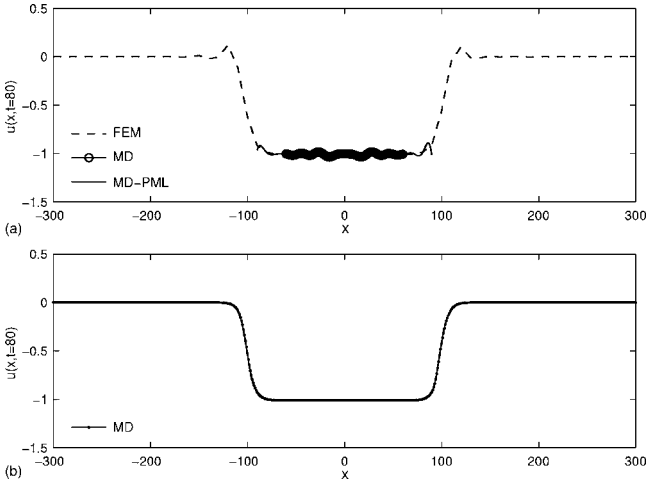

FIG. 9. Displacement at $t=80$ for the 1D lattice problem with sine-Gordon potential function obtained by (a) PMMS and (b) full MD simulation.

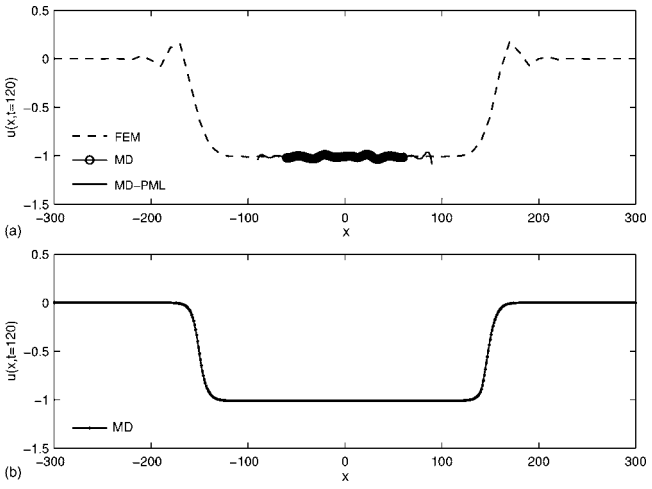

FIG. 10. Displacement at $t=120$ for the 1D lattice problem with sine-Gordon potential function obtained by (a) PMMS and (b) full MD simulation.

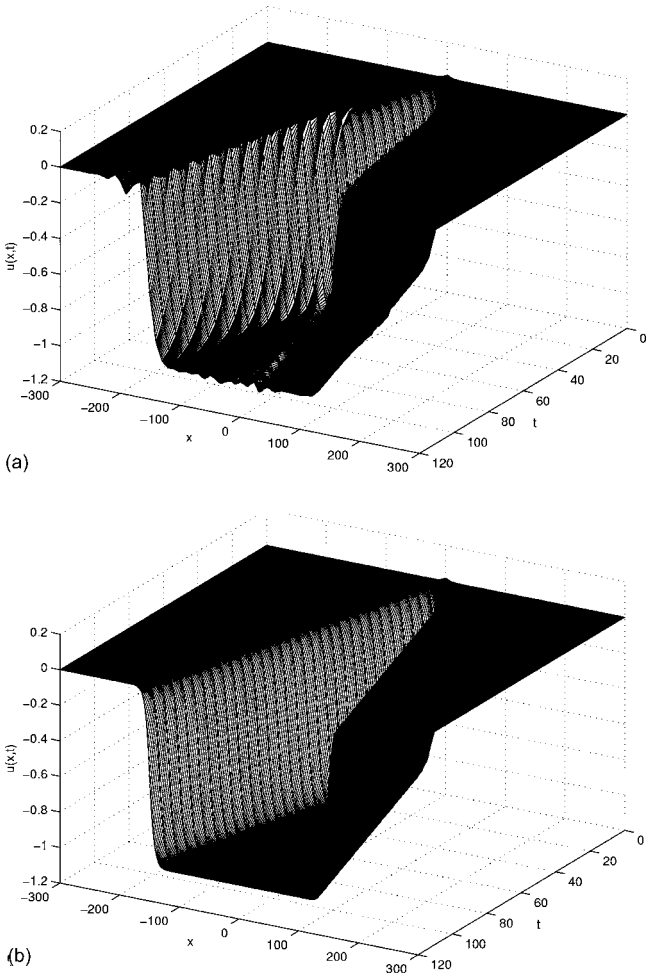

FIG. 11. Time-displacement history for the 1D lattice problem with sine-Gordon potential function obtained by (a) PMMS and (b) full MD simulation.

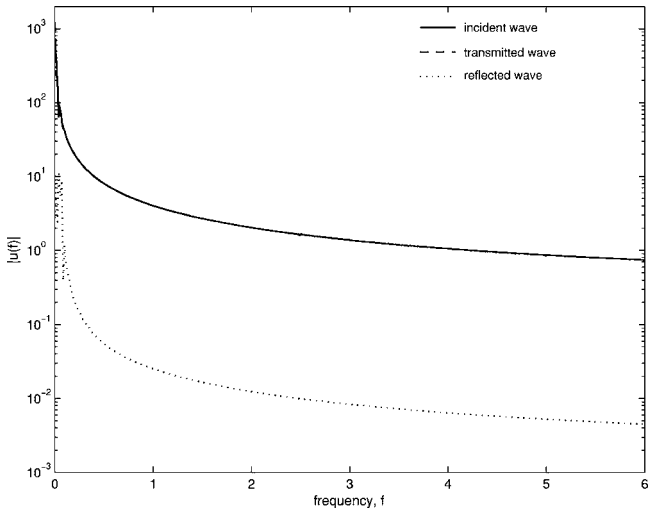

FIG. 12. Fourier spectrum of the incident wave in the pure MD region, the reflected wave in the pure MD region after reaching the handshake region, and the transmitted wave in the FE region corresponding to the sine-Gordon potential example.

the previous example except that the atomic spacing is taken as unity in this example. The fine and coarse time steps are chosen as follows: $\Delta t_m=0.04$ and $\Delta t=0.4$. The values used for the parameters in Eqs. (42) and (43) are $x_0=0.02$, $b=0.2$, and $\beta=0.2$.

Figures 8–10 show the displacement distribution at various coarse time steps: $t=40$, $t=80$, and $t=120$, respectively. The time-displacement histories obtained from both PMMS and full MD simulation are displayed in Fig. 11. Similar to the previous example, the solution of PMMS smooths out the sharp features that exist in full MD simulation, and there is still a small number of waves being reflected back into the MD region. A Fourier spectral analysis of the incident wave, reflected wave, and transmitted wave is performed, and its results are shown in Fig. 12. The displacement-time histories of the incident wave and the reflected wave are measured at $x=30$ in the MD region and that of the transmitted wave is measured at $x=100$ in the FE region. The energy of the incident wave decays almost monotonically with an increase in frequency. The incident wave and the transmitted wave Fourier spectrum is almost identical. Similar to the Lennard-Jones potential example, the reflected wave is approximately two orders of magnitude less than the incident wave in amplitude, but their frequency content is similar.

VI. CONCLUDING REMARKS

Both the idea and implementation of the perfectly matched multiscale simulations (PMMS) are simple. Only the local heterogeneous region is modeled by using the MD simulation, while the rest (but vast area) of the medium is modeled by quasi-continuum approach. To match the MD simulation and quasi-continuum modelings, the perfectly matched layer (PML) is employed to absorb outgoing transient waves from the MD zone, which leaves very few artificial reflections back into the MD region. With the PML, impedance force or matching boundary conditions at the

outer boundary of the MD region are not needed for PMMS as required in some other multiscale methods.[1,2,6] As a matter of fact, the PML can also be thought of as another way to impose matching atomistic/continuum boundary conditions, but, clearly, the advantages in utilizing the PML are its generality and flexibility.

We would like to point out that the PML/MD interface reflection coefficient used in this paper has not been optimized yet. To derive optimal reflection matching coefficients at the atomistic/continuum interface, which balance numerical accuracy, efficiency, and stability, is still a task on hand. We do not anticipate any major problems in doing so, because this and other issues, e.g., extending the PMMS to multiple dimensions, have been well understood and have been resolved in solving various other types of differential equations.[11–14]

The proposed method has not been thermalized in this work, but one may design a thermodynamics-based PML reflection coefficient, for instance, one can let,

$$\tilde{d}(x_p,T)=\left(\frac{T_0}{T}-1\right)d(x_p), \tag{44}$$

where T_0 is the temperature of the heat bath and T is the temperature of the MD region. By doing so, the PMMS algorithm may preserve thermodynamic equilibrium.

On the other hand, the projector obtained from the multiscale decomposition for mapping the MD displacement to coarse scale displacement may also play a significant role in the accuracy of the method. These topics will be addressed in separate works.

ACKNOWLEDGMENTS

This work is supported by a grant from NSF (Grant No. CMS-0239130), which is greatly appreciated.

*Electronic address: li@ce.berkeley.edu

[1] W. Cai, M. deKoning, V. V. Bulatov, and S. Yip, Phys. Rev. Lett. **85**, 3213 (2000).
[2] W. E and Z. Huang, Phys. Rev. Lett. **87**, 135501 (2001).
[3] W. E and Z. Huang, J. Comput. Phys. **182**, 234 (2002).
[4] W. E, B. Engquist, and Z. Huang, Phys. Rev. B **67**, 092101 (2003).
[5] W. K. Liu, E. G. Karpov, S. Zhang, and H. S. Park, Comput. Methods Appl. Mech. Eng. **193**, 1529 (2004).
[6] G. J. Wagner and W. K. Liu, J. Comput. Phys. **190**, 249 (2003).
[7] G. J. Wagner, E. G. Karpov, and W. K. Liu, Comput. Methods Appl. Mech. Eng. **193**, 1579 (2004).
[8] H. S. Park, E. G. Karpov, P. A. Klein, and W. K. Liu, Philos. Mag. **85**, 79 (2005).
[9] J. Berenger, J. Comput. Phys. **114**, 185 (1994).
[10] J. Knap and M. Ortiz, J. Phys. Mech. Solids **49**, 1899 (2001).
[11] E. Turkel and A. Yefet, Appl. Numer. Math. **27**, 533 (1998).
[12] Y. G. Zeng and Q. H. Liu, J. Acoust. Soc. Am. **109**, 2571 (2001).
[13] L. Dedek, J. Dedkova, and J. Valsa, IEEE Trans. Magn. **38**, 501 (2002).
[14] F. Hu, J. Comput. Phys. **173**, 455 (2001).
[15] F. Collino and C. Tsogka, Geophysics **66**, 294 (2001).
[16] W. K. Liu and T. Belytschko, Comput. Struct. **15**, 445 (1982).